Physicochem. Probl. Miner. Process., 56(1), 2020, 204-218

http://www.journalssystem.com/ppmp

Physicochemical Problems of Mineral Processing

ISSN 1643-1049

Received September 10, 2019; reviewed; accepted December 12, 2019

Selective leaching of copper from near infrared sensor-based pre-concentrated copper ores

Amos Idzi Ambo [1,2], Shekwonyadu Iyakwari [3], Hylke J. Glass [1]

[1] Camborne School of Mines, University of Exeter, Penryn TR10 9FE, Cornwall, UK

[2] Department of Chemistry, Federal University of Lafia, P.M.B. 146, Lafia, Nigeria

[3] Department of Geology, Federal University of Lafia, P.M.B. 146, Lafia, Nigeria

Corresponding author: shekwo.i@science.fulafia.edu.ng (Shekwonyadu Iyakwari)

Abstract: Copper oxide ore was pre-concentrated using near infrared sensor-based method and classified as product, middling and waste. The product and middling fractions were leached with ammonium chloride reagent. The effect of temperature, ammonium chloride concentration, solid- liquid ratio, stirring speed and particle size experimental variables were investigated. Mineralogical and chemical analysis of the ore fractions indicated that copper content was in accordance with the pre-concentration strategy, with the product having a higher concentration than the middling and waste. The rate of copper extraction was found to be higher in the product than in the middling sample which further supports the near infrared classification, QEMSCAN®, X-ray diffraction, SEM mineralogical and X-ray florescence and Inductively coupled plasma Mass spectrometry chemical data. It was revealed that the leaching rate increases with increasing ammonium chloride concentration, temperature and decreasing ore particle size, stirring speed and solid-liquid ratio. Analysis of the experimental data by shrinking core model indicated that the dissolution kinetics follow the heterogeneous reaction model for the chemical control mechanism where the activation energies of 45.9 kJ/mol and 47.5 kJ/mol for product and middling fractions respectively were obtained. Characterization of the residue obtained at optimum leaching condition with X-ray diffraction suggests that copper was selectively leached when compared to the profile of the raw ore. The trace levels of metals associated with abundant X-ray diffraction profiles of residue found in the leachate further confirm the selective leaching process.

Keywords: near infrared, leaching, pre-concentration, ore characterization, copper

1. Introduction

The processing of copper metal from low grade resources has continued to be a challenge due to the gradual depletion of high grade copper ore resources, which has steadily given rise to low copper grades from mined ores (Sun et al., 2009). The major problem associated with processing of low grade copper ores is their high gangue contents. The high gangue content increasingly makes the processing of such deposits difficult. Furthermore, their complex nature and significant concentrations of undesirable metals such as Fe, Co, Mn, Pb, Zn, As and Ni, also leads to high processing costs (Awe, 2013).

Ore containing high concentration of calcite are considered problematic due to their high consumption of H_2SO_4 acid leading to additional lixiviant requirement (Bingöl and Canbazoğlu, 2004). Since H_2SO_4 is often used for leaching of most copper ores, the viability of the application of the reagent depends on the nature of the ore (Sun et al., 2009). According to Bingöl et al. (2005), acid consumption in copper oxide ore during leaching ranges from 0.4 to 0.7 tonne per tonne of copper recovered. Also, Bingöl and Canbazoğlu (2004) found that 9.8 kg of the acid is usually consumed by 1 percent calcite during leaching. Therefore, the presence of calcite as gangue in significant amount in copper ores could render such ore unsuitable for processing with H_2SO_4.

DOI: 10.5277/ppmp19098

Besides the concerns of consumption by calcite of H_2SO_4, the reagent is aggressive with poor selectivity for copper, leading to the excessive dissolution of certain metals: Fe, Mn, Pb, Co, from the ore matrix into the leachate solution as impurities. The presence of these metals in the leachate usually result in additional processing cost in the downstream processing for copper recovery (Ekmekyapar et al., 2003; Künkül et al., 2013; Awe, 2013). These impurities have negative impact on the quality of copper metal produced unless removed (Fillipou et al., 2007). The processes for removing these impurities from the leachate usually result in high capital expenditure, the development which leads to growing interests in the elimination of impurities before leaching and during leaching before electrowinning (Larouche, 2001, Awe and Sandström, 2010).

The only way to overcome the high cost of processing is to develop methods capable of reducing the gangue content and concentration of other metals in ores before or during leaching (Meech and Paterson, 1980; Liu et al., 2010). The focus is on the development of techniques that are capable of minimising the amount of undesirable materials going to the downstream processing. This can only be achieved through innovative technologies (Wills and Napier-Munn, 2006).

It is imperative to overcome the high cost of processing low grade ores by developing methods capable of reducing high gangue content in ores by pre-concentration before subjecting same to the leaching stage for maximum output of the process (Iyakwari et al. 2016). Chemical reagents with high selectivity for copper during leaching have been shown to be alternatives to H_2SO_4 acid reagent (Popescu et al., 2013). Premium is now placed on alkaline lixiviants due to their low leaching kinetics with high selectivity for copper from high gangue carbonates and silicates ores (Meech and Paterson., 1980; Wang et al., 2009; Norgate and Jahanshahi, 2010; EKmekyapar et al., 2012; Ochromowicz et al., 2014). Some of the perceived advantages of alkaline lixiviant in the leaching of ore sources are reduced dissolution of Fe and ease of purification (Chmielewski et al., 2009; Liu et al., 2012b; Künkül et al., 2013). In many cases, combinations of two or more techniques for copper processing have proven to be efficient for economic recovery from high gangue ores (Wills, 2011).

In the current research an integrated approach was used for processing an ore containing copper with high proportion of silicate and calcite gangue in complex assemblage of other minerals. The two steps approach includes Near InfraRed (NIR) sensor-based pre-concentration and classification of the ore and selective leaching of the classified ore with alkaline lixiviant. The objective of the work therefore, is to investigate the selectivity of the leaching process for copper from the pre-concentrated ore using NH_4Cl and evaluating the leaching kinetics for developing an integrated process for extracting copper from low grade ores.

2. Materials and methods

Copper ore was sampled from a mine in the Los Pozos mining district in the Coastal Range of the Atacama Region, northern Chile. Samples were characterised, pre-concentrated and classified into product, middling and waste using NIR sensor-based technique (Iyakwari et al. 2016). For particle size fraction analysis, the classified ore particles were crushed separately with a Retsch steel jaw crusher (to -3 mm), milled with a tungsten-carbide mill, homogenised and then sieved to obtained the following size fractions: -125/+90 µm, -90/+63 µm and -63/+45 µm.

2.1. Near infrared pre-concentration

The NIR line scanner at Camborne School of Mines (CSM) measures each spectrum at a dimension of 0.29 by 0.9 cm. Individual samples were an average size of between 2 and 2.7 cm. In order to properly map each sample, individual samples were divided into three sectors measuring 0.9 cm each corresponding to NIR spectrum height, with width measuring 0.29 cm (Figure 1). Therefore, the number of spectra produced by individual samples per sector depended on particle size and shape (Iyakwari et al. 2016). Details on NIR background, procedure of NIR data acquisition, instrumentation and data pre-treatment are described in Iyakwari et al. (2013) and Iyakwari and Glass (2015).

2.1.1. Samples NIR spectral correlation and interpretation

The NIR strategy employed was targeted at eliminating both calcite and clay (muscovite/kaolinite) rich particles as gangue. Hence, samples were classified into three groups (Iyakwari et al. 2016):

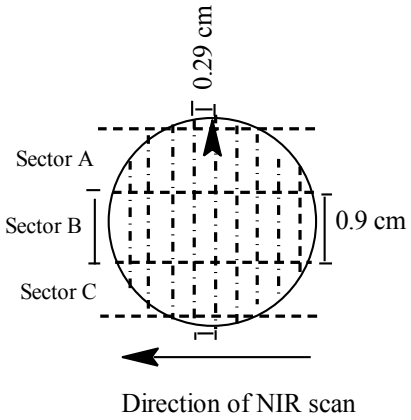

Fig. 1. Samples marked for directional scanning and spectra/mineral mapping (After Iyakwari et al. 2016)

i. Products - the samples with all NIR spectra showing chrysocolla and or hematite, chlorite, biotite pattern. This group includes featureless NIR spectra.
ii. Waste - the samples with all NIR spectra showing calcite and or muscovite characteristic features.
iii. Middlings – the samples with NIR spectra containing individual spectra of both waste and product groups. This is likely since individual mineral grains are smaller than the pixel size of 2.9 by 9 mm, and particles scanned consisted of at least two pixels (which may be distinct). This group may require further liberation to a size not less than the pixel size and rescanned.

2.1.2. Individual sample NIR spectra mapping

Three representative samples one from each class (Figures 2, 3 and 4), representing products, middling and waste respectively are described here in detail. Major absorption features, absorption wavelength position, correlation with reference spectra, and the possible mineral(s) responsible for the absorption features are correlated with mineral data and field scan images.

Product sample generated a total of 22 NIR spectra, corresponding to 8, 8, and 6 spectra per sector scanned (Figure 2 (a, b and c)). Spectra display no absorption feature(s).

A total of 26 spectra were generated from scan of middling sample (Figure 3(a, b and c)). Spectra of sectors A and B displayed no features, while spectra of sector C shows strong mineralogical variation with spectrum number 1, 2, 3, and 4 showing no absorption features, while spectrum number 5, 6, 7, 8 and 9 all showed features near 1410, and 2200 nm. The features displaying spectra also exhibited relatively higher reflectance compared to those without features. The position of features near 1410, and 2200 nm corresponds to muscovite features (Iyakwari et al., 2013).) The featureless spectra correspond to hematite dominated spectra. Muscovite displays diagnostic absorption features in spectrum number 5, 6, 7, 8, and 9. This indicates that muscovite is concentrated more around those spectra. This is confirmed by the sample NIR-active minerals field scan image (Figure 3d). The sample field scan image also reveals that the sample has a porphyritic texture, showing a highly zoned concentration of hematite with patches of muscovite to the lower left of the image.

Spectra of waste sample (Figure 4 (a, b and c)), display characteristic muscovite and calcite features near 1415, 2210 and 2345 nm. Spectra also display high reflectance, which is indicative of absence or low hematite concentration in the sample (Iyakwari et al., 2016). A total of 22 spectra were generated from the scan corresponding to 7, 8, and 7 spectra per sector. NIR-active minerals field scan image of sample (Figure 4d) show both calcite and muscovite occurring almost in same space and time.

2.2. Compositional analysis

2.2.1. Mineralogical analysis

The mineralogical analysis of the pre-concentrated copper ore (product, middling and waste) was carried out with QEMSCAN® 4300 system, which is based on a Zeiss scanning electron microscope.

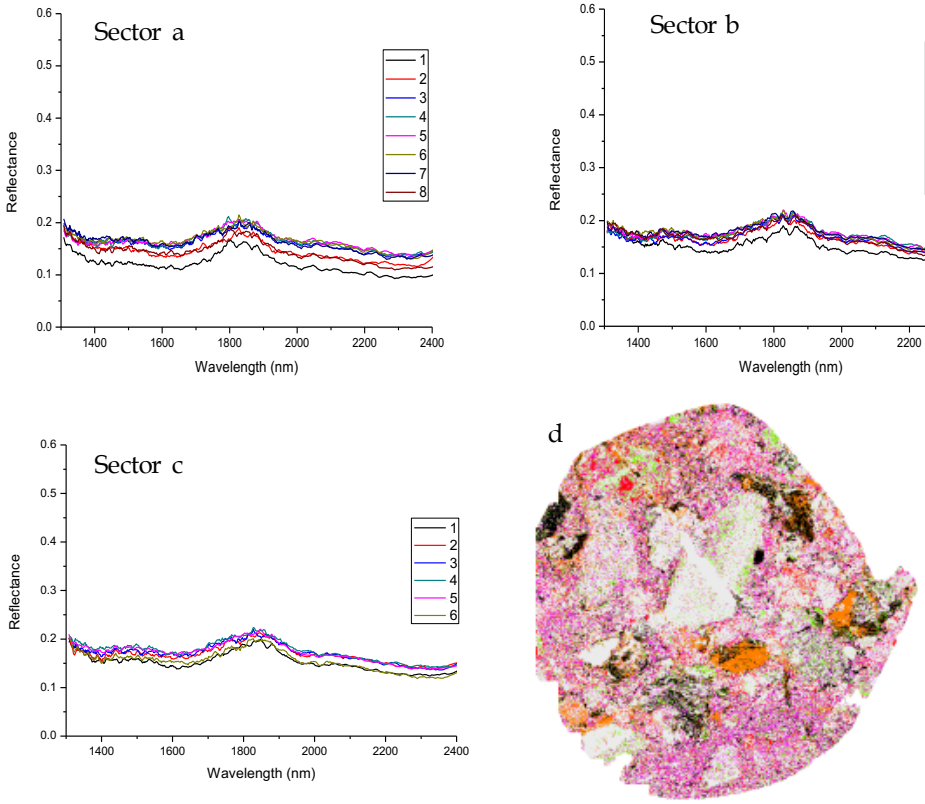

Fig. 2. (sectors a, b and c) –NIR spectra of product sample While d is the QEMSCAN® fieldscan image of sample at 10 μm X-ray resolution, showing only NIR active minerals present in the sample

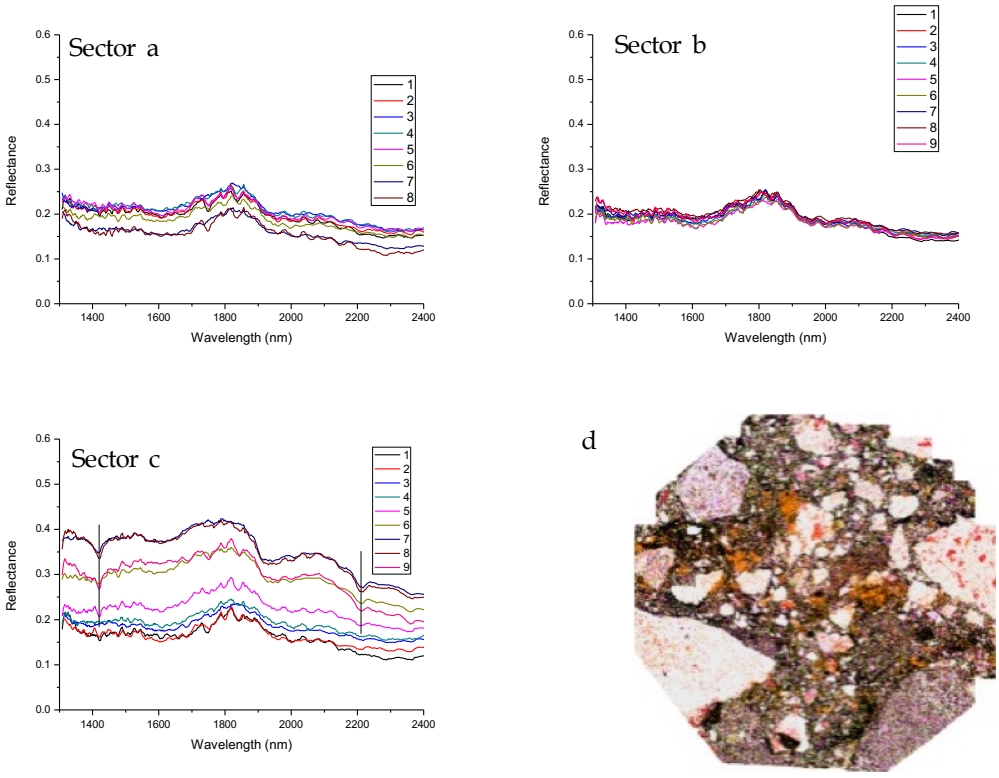

Fig. 3. (sectors a, b and c) NIR spectra of waste sample. While d is the QEMSCAN® fieldscan image of sample at 10 μm X-ray resolution, showing only NIR active minerals present in the sample

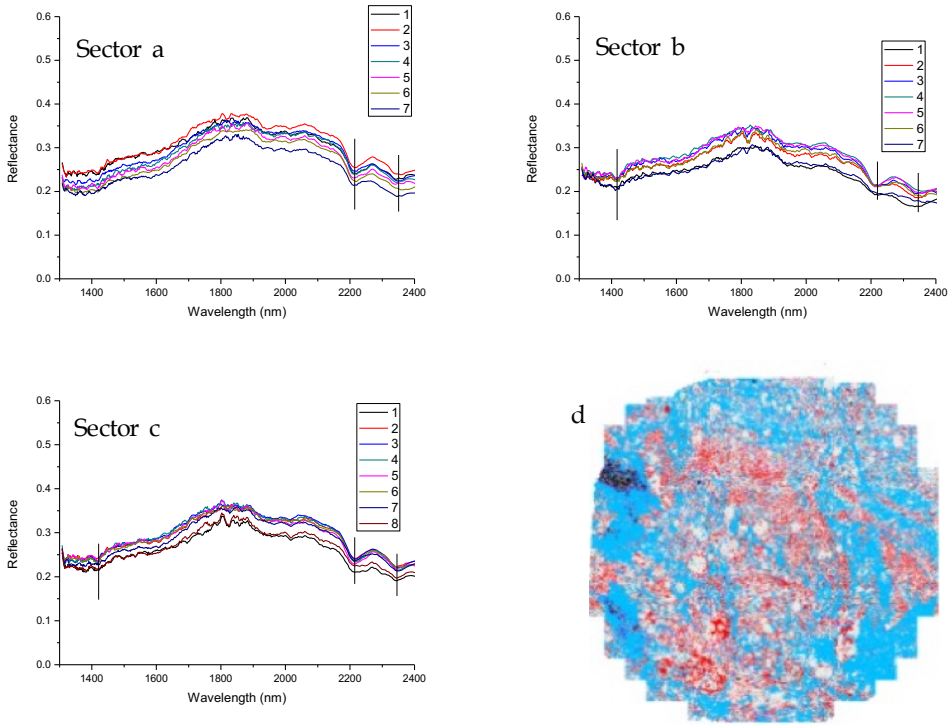

Fig. 4. (sectors a, b and c) NIR spectra of waste sample. While d is the QEMSCAN® fieldscan image of sample at 10 µm X-ray resolution, showing only NIR active minerals present in the sample

A Siemens Bruker D500 XRD analyser (www.bruker.com) with a detection limit of 5% was used to semi-quantitatively measure the mineralogical composition of the ore. XRD measurements were matched with known mineral signatures using Bruker EVA software.

2.2.2. Chemical/textural analysis

Elemental composition of the classified ore samples was measured using portable desktop thermo scientific Niton FXL 950 FM X-Ray Fluorescence analyser (XRF, www.nitonuk.co.uk). The Portable XRF (PXRF) analyser employs Energy Dispersive Spectrometry (EDX) method. The measuring window covers a diameter of 8 mm, and X-rays penetrates approximately 1 to 2 mm into the sample.

Scanning Electron Microscope (SEM) was used to observe ore characteristics such as texture, size and liberation sizes in relation to copper. Polished blocks of-63/+45 µm samples were coated with carbon to improve imagery and enhance surface conductivity. The SEM equipment used for the analyses was a JEOL JSM-5300LV Low Vacuum SEM equipped with EDS ISIS software.

The metal grades of the pre-concentrated and classified ore were determined with Inductively Coupled Mass Spectroscopy (ICP-MS, Agilent Technology, Model 7700). Samples were first digested by dissolving the fractions in Aqua regia (75% 6 N HCl and 25% 15.8 N HNO_3) at 90 ˚C for 1 h. 50 times dilution of leachate was carried out with 50% HNO_3 prior to determination with ICP-MS.

2.3. Leaching operation

The leaching experiments were performed in 500 mL reactor with a four-neck split flask in a thermostatically heating mantle with a temperature control unit. The reactor is designed with an overhead mechanical stirrer for agitation and a rubber stopper for sampling of leachate. The desired temperature for leaching is obtained by adjusting the thermostatically-controlled electric heating mantle. For each experimental run, 250 mL of freshly prepared aqueous solution of NH_4Cl of known molarity was charged into the reactor and heated to the required temperature before adding the solid copper ore sample. The reactant was stirred at a desired stirring speed and reaction temperature attained. 5 mL of leachate solution was withdrawn at time interval of between 15 to 240 minutes, filtered using Whatman filter paper and filtrate determined for dissolved metals. The experiment was mostly carried out with particle size of -63/+45 µm except otherwise stated. The fraction of metal dissolved

was calculated from the head grade. Selected residue obtained after optimum leaching were oven-dried at 40 ˚C for 5 days and analysed for metal contents with ICP-MS while the other portion determined for selective extraction using XRD technique. All reagents used were high purity analytical grade purchased from VWR Chemical Company, UK and used with de-ionised water without further purification. Experimental condition for the leaching experiment is shown in Table 1.

Table 1. Experimental variables and their ranges

Variables	Values		
NH_4Cl concentration, M	0.55,	1.0,	1.65*
Particle size fraction, µm	-63/+45*,	-90/+63,	-125/+90
Solid to liquid ratio, g/L	6/250*,	7/250,	8/250
Agitation speed, rpm	300*,	500,	800
Temperature, ˚C	70,	80,	90*

*optimized parameters

3. Results

3.1. Characterization studies of pre-concentrated ore

3.1.1. Mineralogy characterization

QEMSCAN® mineralogical analysis shown (Table 2) indicated that the pre-concentrated and classified ore contained the following minerals in different proportions: hematite, and cuprite (oxides), calcite, and malachite (carbonates). Others are chrysocolla, muscovite, biotite, kaolinite, chlorite, K-feldspar and quartz, (silicate), and apatite (phosphate). The major copper-bearing mineral in the ore is chrysocolla, with the product fraction having more chrysocolla concentration than the middling and waste. Malachite and cuprite are the other copper bearing minerals in the ore, all occurring in minute concentration. Except these three minerals, the remaining are here considered gangue mineral. Of these gangue groups, the quartz, muscovite, kaolinite, chlorite and the K-feldspars constitute the most significant concentration. Same can be said of calcite which is a carbonate mineral. In terms of gangue mineral content in the classified ore, the concentration is waste > middling > product (Table 2).

XRD analysis (Figures 5 to 7) showed that hematite (oxide), calcite (carbonate) muscovite, clinochlore (chlorite), quartz, biotite, microcline (K-feldspar), and orthoclase (K-feldspar) (silicates) as the only minerals with concentration above 5 %. Amorphous minerals were also inferred from profile showing a rise in baseline with increase in the 2-Theta value (Iyakwari et al. 2016).

Table 2. Mineralogical analysis of NIR sensor-sorted ore samples with Qemscan®, in wt-%

Sample ID	Chrysocolla	Hematite	Cuprite	Muscovite	Biotite	Kaolinite	Malachite	Chlorite	Calcite	K-feldspar	Quartz
Product	3.93	23.92	0.01	2.89	10.92	0.11	0.17	11.67	2.87	27.50	14.11
Middling	2.70	48.75	0.00	3.20	4.98	0.54	0.00	6.63	1.73	14.11	15.23
Waste	0.73	1.47	0.02	4.06	7.38	0.01	0.17	20.66	12.10	15.63	34.08

3.1.2. Chemical characterization

The elemental analysis of the classified ore fractions (-125/+90 µm, -90/+63 µm and -63/+45 µm) by XRF in Table 3 indicated that the NIR sensor-based pre-concentration led to discrimination of copper

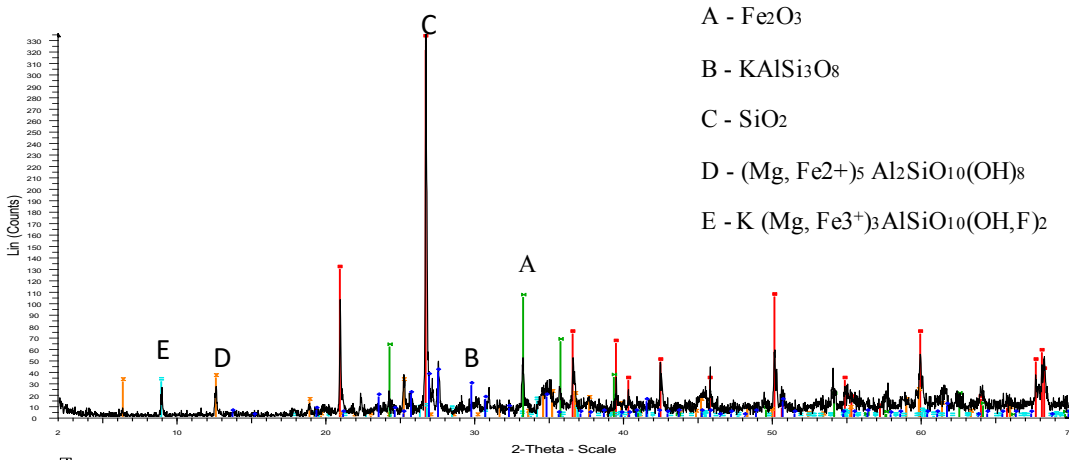

Fig. 5. XRD profile of product sample

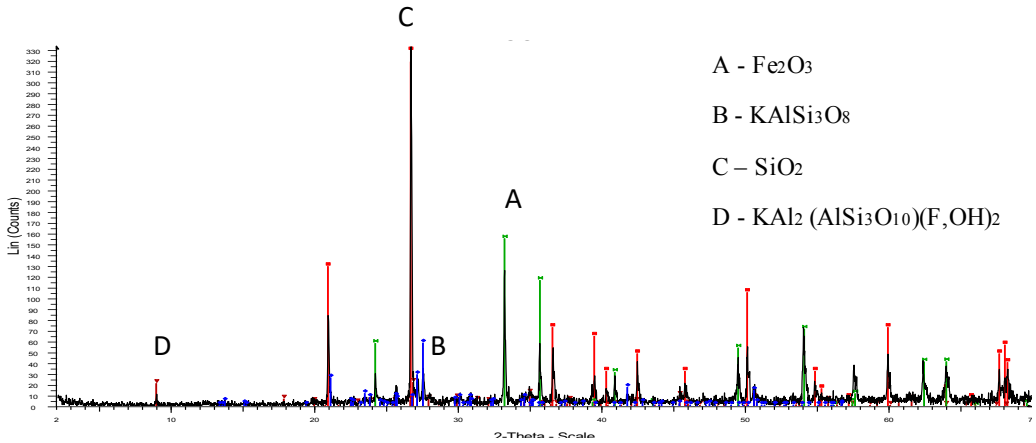

Fig. 6. XRD profile of middling sample

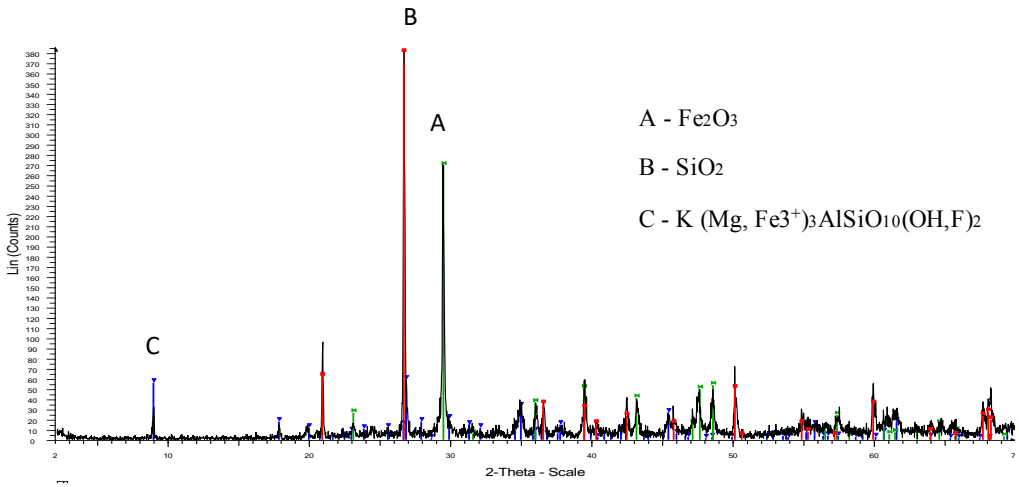

Fig. 7. XRD profile of waste sample

ore with significant variation in metal grades. The Cu concentration increases from waste, middling to product, thus, agreeing with the NIR classification. Also observed is the increase in copper grade with increasing particle size. The waste fraction contained the highest calcium grade, while the lowest was found in the product. The concentration of Fe was higher in the middling than in the product and the waste. The trend of increasing Fe concentration was observed with decreasing particle size in the middling and waste fractions.

Table 3. XRF analysis of product, middling and waste fractions, in wt-%

Particle size range, µm	Cu	Ni	Co	Fe	Mn	Zn	Ba	Cr	V	Ti	Ca	K	Al	P	Si	Residue
							Product									
−125+90	1.82	0.01	0.03	36.2	0.05	0.05	0.05	0.04	0.04	0.26	0.22	2.12	2.3	0.27	7.9	48.5
−90+63	1.73	0.01	0.03	38.2	0.05	0.05	0.03	0.04	0.04	0.27	0.24	2.05	2.2	0.27	7.8	46.9
−63+45	1.56	0.01	0.04	42.2	0.05	0.04	0.02	0.04	0.04	0.25	0.25	1.81	2.1	0.27	7.5	43.7
							Middling									
−125+90	0.33	0.03	0.05	52.8	0.00	0.00	0.02	0.04	0.04	0.08	1.60	0.93	1.5	0.26	5.1	37.1
−90+63	0.34	0.03	0.06	53.3	0.00	0.00	0.02	0.04	0.04	0.09	1.61	0.90	1.5	0.27	5.0	36.6
−63+45	0.32	0.04	0.06	55.6	0.11	0.00	0.03	0.04	0.04	0.09	1.55	0.82	1.6	0.26	4.8	34.7
							Waste									
−125+90	0.07	0.00	0.00	8.20	0.13	0.13	0.10	0.02	0.03	0.27	5.25	3.83	2.2	0.38	10	68.4
−90+63	0.07	0.00	0.00	9.20	0.13	0.12	0.09	0.02	0.03	0.28	5.94	3.76	2.1	0.38	10	67.2
−63+45	0.07	0.00	0.00	10.0	0.13	0.12	0.09	0.02	0.03	0.30	6.12	3.86	2.3	0.39	10	65.9

Metal grade determined with ICP-MS is presented in Table 4. Only two classified ore fractions (product and middling) were analysed. The available Cu for leaching increases with decreasing particle size fraction. This suggests that the higher surface area of finer particles (-63/+45 µm) makes it more amenable to leaching. It was found that the variation in the trend of metal grade between the XRF and ICP-MS was due to the differences in the methods of sample preparation and or measurement.

Table 4. Metal grades determined with ICP-MS

Sample category	Particle size range	Cu (wt. %)	Zn (ppm)	Mn (ppm)	Co (ppm)	Ni (ppm)
Product	−125+90 µm	1.04	0.01	0.04	0.00	0.00
	−90+63 µm	1.70	0.01	0.05	0.00	0.00
	−63+45 µm	1.79	0.02	0.06	0.03	0.01
Middling	−125+90 µm	0.70	0.01	0.01	0.01	0.00
	−90+63 µm	0.72	0.02	0.02	0.01	0.00
	−63+45 µm	1.01	0.02	0.02	0.03	0.02

The -63/+45 µm was characterise with Scanning Electron Microscope (SEM) to observe the shape, texture and liberation sizes in relation to Cu. It was found that the Cu is interlocked with other metals in the ore matrix (Figure 8). The SEM image obtained indicated that the copper particles in the crushed ore are finely disseminated, the ore is morphologically characterised by intergrowth with chrysocolla minerals hosting copper particles residing within the hematite rich iron source and K-feldspars. This confirms the assertion by Mena and Olson (1985) on the characteristic porous nature of the chrysocolla minerals. The observed phenomenon could be due to absorption of elements by chrysocolla. The analysis of classified ore revealed spatial variability within the crushed ore with copper ubiquitously distributed within the crushed grain sizes of the chrysocolla, K-feldspar and hematite. Also, due to the presence of calcite (high acid consuming gangue) in the ore, it requires liberation to fine particle sizes. The same observation was obtained for both middling and product with the difference been in the

variations in concentrations of Fe-Cu as shown by their EDX (Figure 9). A model revealing the porous nature of the ore and metal distribution within the ore matrix is represented in Figure 10. The figure indicated micro cracks and pores in the material which is in line with the nature of the ore material.

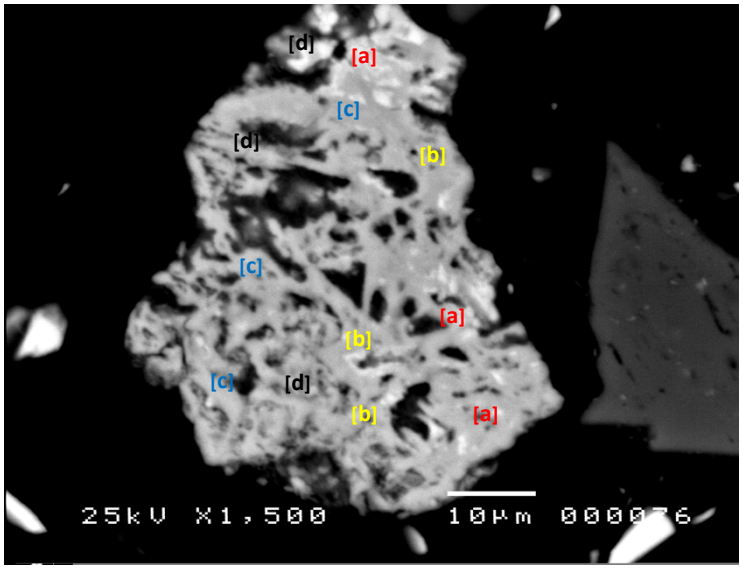

Fig. 8. BEI SEM image of polished block. [a] Cu, $Al)_2H_2Si_2O_5(OH)_4.n(H_2O$, [b] Fe_2O_3, [c] $KAlSi_3O_8$, [d] SiO_2 (product fraction)

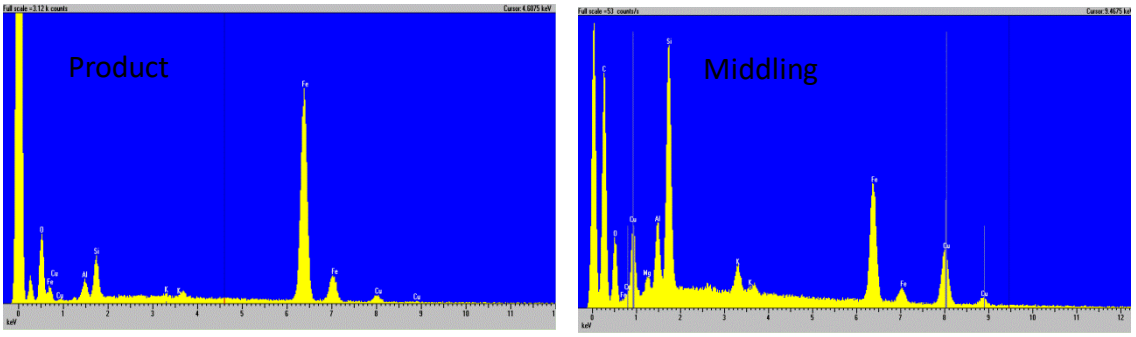

Fig. 9. EDS of product and middling indicating Fe-Cu concentration in the ore

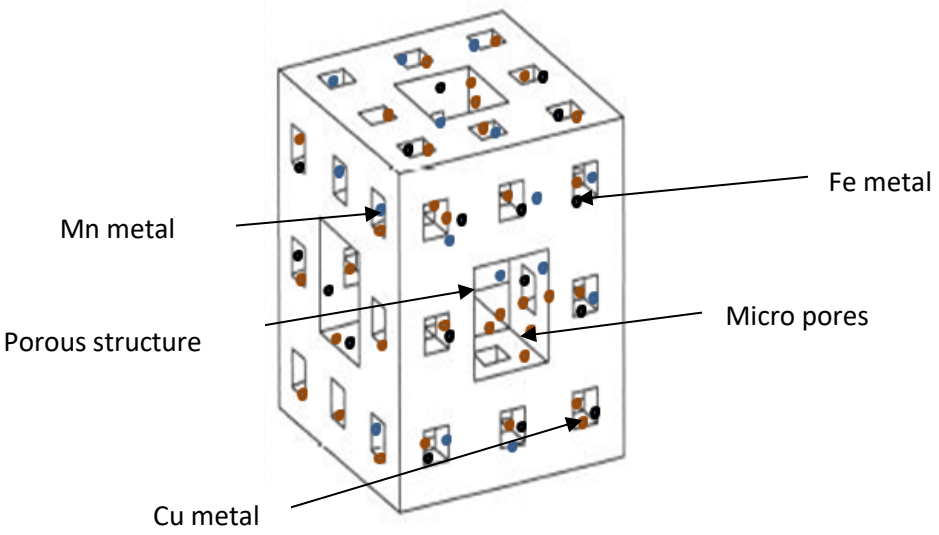

Fig. 10. Model showing some metal distribution within the product and middling ore fraction

3.2. Effect of leaching variables

3.2.1. Effect of temperature

The effect of reaction temperature on the Cu extraction rate of the pre-concentrated copper ores was studied at temperature ranges of 70 ˚C, 80 ˚C and 90 ˚C. In each case, other experimental variables: stirring speed, NH_4Cl concentration and particle size were kept constant (Table 5). Figure 11 shows that higher leaching rates were obtained with increase in reaction temperature. The observed behaviour supports the fact that temperature accelerates and enhances the rate of Cu extraction into the leaching media. This occurs as a result of the increase in reaction velocity constant k between the reactants. Higher leaching rate was obtained with the product due to the high Cu content compared to the middling. However, similar trend of increasing rate of Cu extraction in both ore category was obtained. Thus, the result is consistent with the NIR pre-concentration and classification.

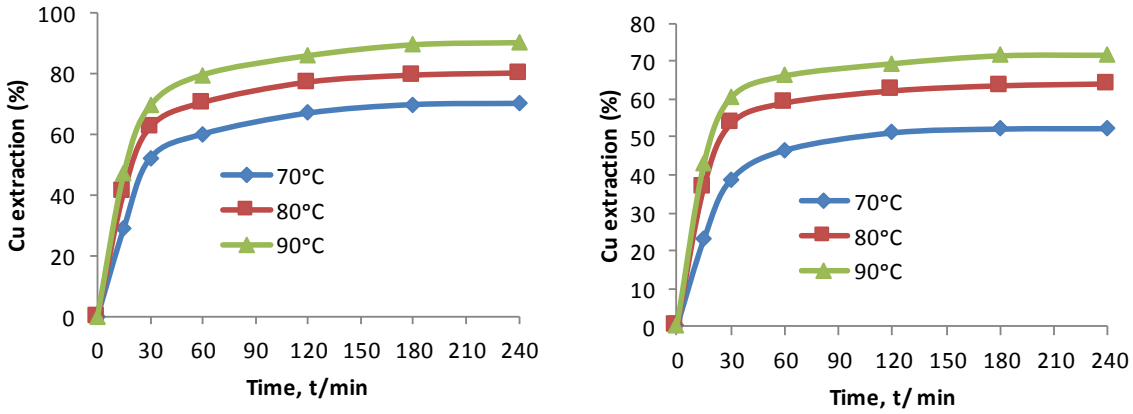

Fig. 11. Effect of reaction temperature on Cu extraction rate

3.2.2. Kinetic analyses

The heterogeneous fluid-solid reaction systems have been applied in hydrometallurgical and chemical reaction processes (Awe, 2013). The shrinking core model was used to investigate the mechanism of the leaching process because of its wide application (Aydogan et al., 2005; Levenspiel, 1999; Baba and Adekola, 2010; Awe, 2013, Baba et al., 2013). The heterogeneous solid-liquid reaction between the ore and NH_4Cl reagent is expressed in Eq. (1).

$$A\ (NH_4Cl\ liquid) + B\ (solid\ Cu\ particle) \rightarrow product \quad (1)$$

The dissolution rate has been found to decrease with time and highly dependent on the activation energy. The experimental data obtained were fitted into the shrinking core models, where the model with high rate constant and coefficient of variation is considered the best model representing the leaching reaction. The following mathematical expressions for diffusion of fluid through the product layer (Eq. 2), surface reaction (chemical-controlled) (Eq. 3) or by mixed controlled process (Eq. 4) with the assumption of a shrinking core particle model shown below were tested:

$$1-\frac{2}{3}\alpha - (1-\alpha)^{2/3} = \frac{2M_S D C_A t}{\rho_s \beta r^2 O} = k_d t \quad (2)$$

$$1-(1-\alpha)^{1/3} = \frac{K_c M_B C_A t}{\rho s \beta ro} t = k_r t \quad (3)$$

$$\alpha = k_f t = \frac{3bk_c C_A}{\rho s ro} \quad (4)$$

where α is the fraction reacted, K_C is the kinetic constant, M_S is the molecular weight of the solid, C_A is the concentration of the dissolved lixiviant A is the bulk of the solution, ρ_s density of the classified ore, β is the stoichiometric coefficient of the reagent in the leaching reaction, ro is the radius of the solid particle, t is the reaction time, D is the diffusion coefficient in the porous product layer, k_r and k_d are rate constant.

The Arrhenius equation (Eq. 5) was used to determine the activation energy of the process.

$$k_r = A \cdot \exp\left[{}^{-Ea}/_{(RT)}\right] \quad (5)$$

where A is the frequency factor, Ea is the apparent activation energy, R is the universal gas constant, and T is the absolute temperature.

The experimental values in Figure 11 were fitted into the models in Equations 2 to 4. Good correlation coefficient was obtained with the model in Eq. (3) and was subsequently used for kinetic analysis and determination of activation energy.

A plot of $1-(1-\alpha)^{1/3}$ vs. leaching time t, for experimental data in Figure 11 is presented in Figure 12. The activation energy of the reaction was calculated by plotting ln(kr) vs. 1/T. The slope of the line in Figure 13 gave the value of E/R and intercept k. The value of E/R was found to be 45.9 Kj/mol for product and 47.5 Kj/mol for middling. The slight variation in activation energy suggests that the middling requires more energy to break the fissures for chemical reaction to take place. These values are indications that the leaching process is chemically-controlled through reaction at the particle surface. This agrees with findings reported by Awe (2013) and Baba et al. (2013).

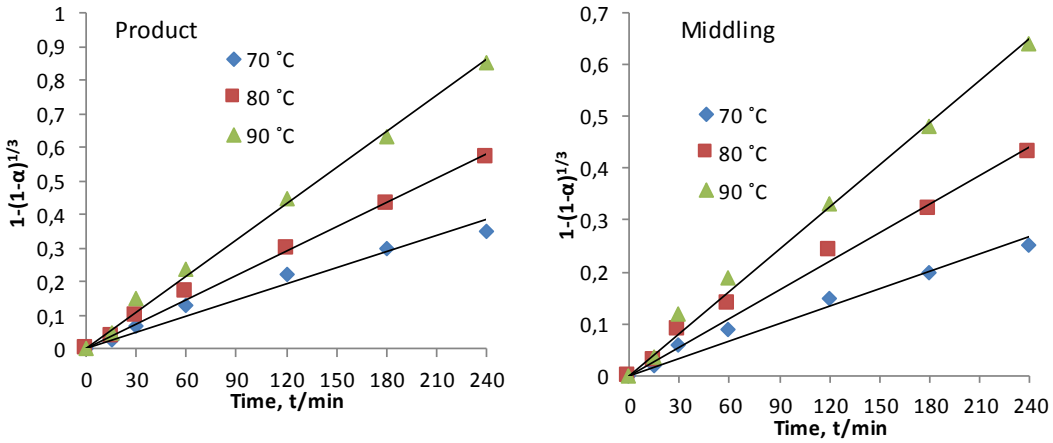

Fig. 12. Plot of $1-(1-\alpha)^{1/3}$ vs. leaching time

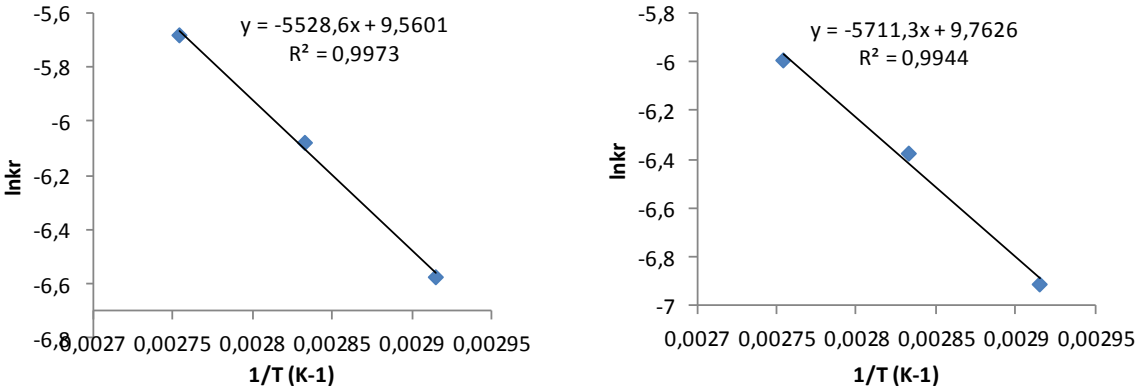

Fig. 13. Arrhenius plot of ln(kr) vs. 1/T

3.2.3. Effect of NH_4Cl concentration

Figure 14 present result of the effect of NH_4Cl on the leaching of pre-concentrated copper ore. The effect of NH_4Cl concentration on the leaching was determined using NH_4Cl concentrations of 0.55 M, 1.0 M and 1.65 M, while the particle size, solid-liquid ration and temperature were kept constant (Table 1). Under the experimental conditions, the rate of Cu extraction increased with increasing NH_4Cl concentration in the pre-concentrated ore categories. The rate of Cu dissolution in the product was far greater than that of the middling across the different concentration ranges. This is to be expected based of the mineralogical and elemental analysis shown in Tables 2 to 4. The experimental data was interpreted using Eqs. (2) – (4). It was found that of all the three models tested, the experimental data fitted well into Eq. (3) with good correlation coefficient (R^2) obtained. Consequently the kinetic data were expressed using Eq. (3) by plotting $1-(1-\alpha)^{1/3}$vs. leaching time for the data in Figure 14. The

experimental rate constants *kr* determined from the slopes in Figure 14 was used to estimate the reaction order. A plot of ln(kr) vs. ln[NH_4Cl] was constructed as shown in Figure 15.

The slope of the resulting plot in Figure 15 gave values of -1.6 and -1.7 representing the reaction order with respect to the $NH4^+$ ion concentration. This is an indication that the leaching process is of the -1.6 and -1.7 -order mechanism.

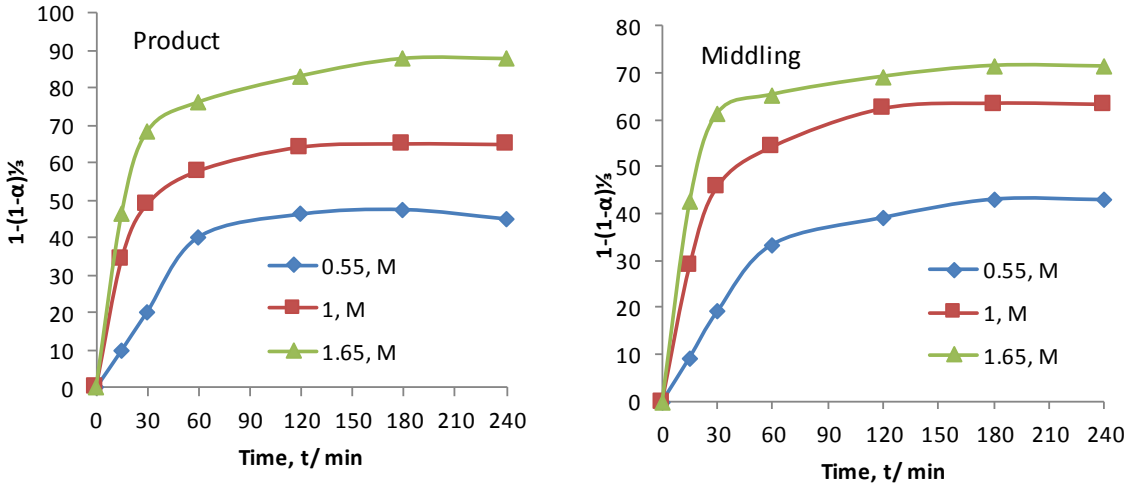

Fig. 14. Effect of NH_4Cl concentrations on Cu extraction rate

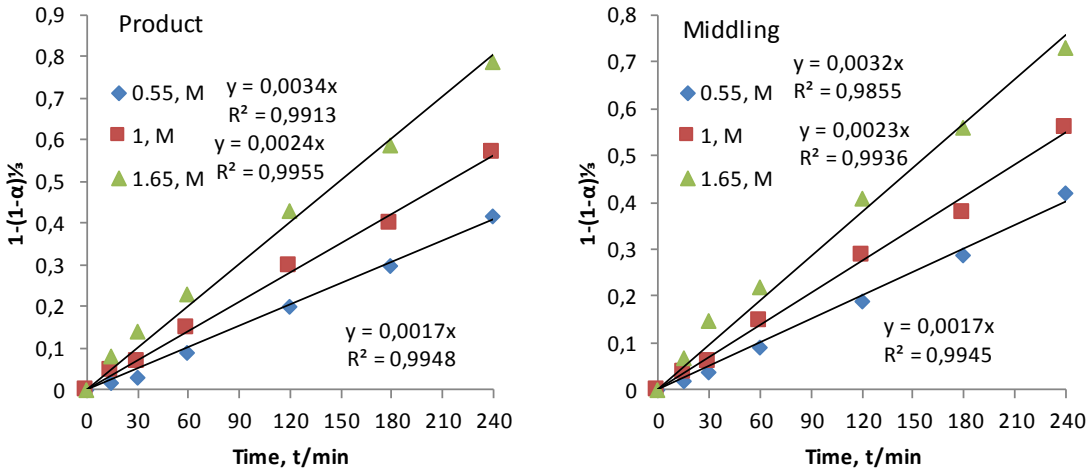

Fig. 15. Plot of 1-(1-α)⅓vs. leaching time (t) for different NH_4Cl concentration

3.2.4. Effect of particle sizes

The effect of particle sizes on the Cu extraction rate rate of the pre-concentrated ore was evaluated by using -125/+90 µm, -90/+63 µm and -63/+45 µm size fractions while the temperature, stirring speed, NH_4Cl concentration and solid-liquid ratio were kept constant at 90 ˚C, 300 rpm, 1.65 M, 6g/250 mL, respectively. Figure 16 shows that the Cu extraction rate increases with decreasing particle diameter due to increased surface area for effective interaction of the reagent with the copper ore. It is also found that higher rates were obtained with the product, although the trend in dissolution is the same.

3.2.5. Effect of stirring speed

Figure 17 shows the influence of stirring speed on the leaching rate of pre-concentrated copper ore. It was found that the rate of Cu extraction decreases with increasing stirring speed from 300 rpm to 500 rpm and 800 rpm when the effect of temperature, NH_4Cl concentration, particle size and solid-liquid ration were kept constant at 90 ˚C, 1.65 M, -63/+45 µm and 6g/250 mL. The values of Cu extraction is an indication that high stirring rate above 300 rpm does not result in increases in Cu extraction, thus high stirring is not required for effective leaching of this ore. It is likely that due to the porous nature of

the material more contact at low stirring speed allows for entry of chemical reagent into the ore matrix. This agrees with findings reported by Baba et al. (2013).

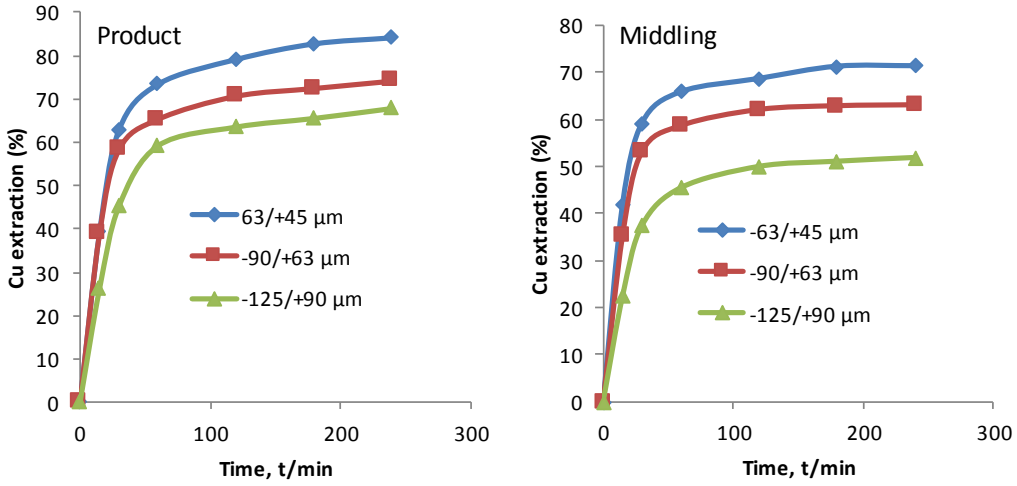

Fig. 16. Effect of particle sizes on Cu extraction rate

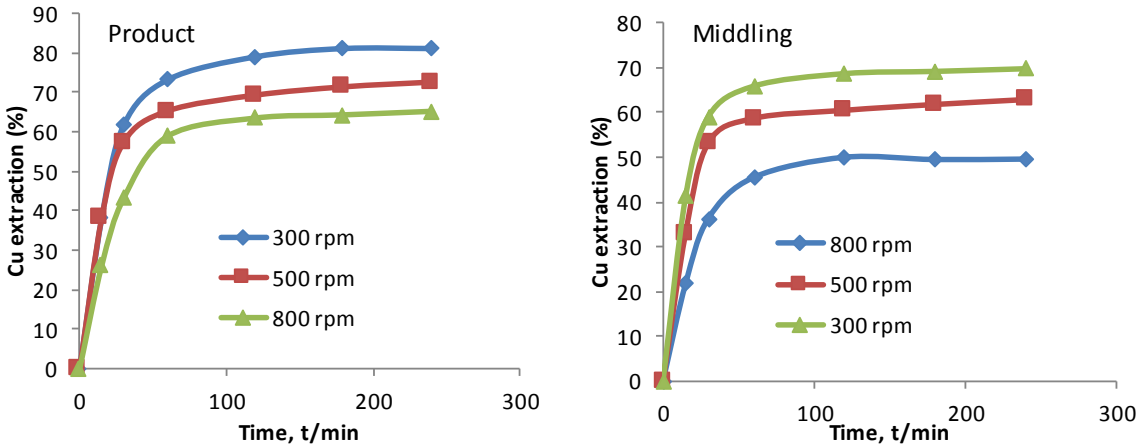

Fig. 17. effect of stirring speed on Cu extraction rate

3.2.6. Residue analysis

Residue obtained at optimum leaching conditions: NH_4Cl concentration 1.65 M, stirring speed 300 rpm, particle size -63/+45 µm, temperature 90 ˚C, solid-liquid ratio 6g/250 mL and leaching time of 240 minutes was characterized using XRD technique. Result of XRD profiles obtained is shown in Figure 18. Comparison of these XRD profiles with those obtained for the raw ore in Figures 5 and 6 reveals the absence of any rise of baseline, which was assumed to be indicative of amorphous minerals (in this research malachite and chrysocolla). Observed in the profile, are hematite, clinochlore, muscovite and quartz peaks, thus indicating that they were not leached. Since these minerals were not leached, it is an indication that they were unreactive toward NH_4Cl lixiviant. Similarly, ICP-MS analysis of leachate and residue for concentration of these metals (Fe, Mn, Zn, Co) which are associated with these minerals shows low traces when compared to that of the raw ore in Tables 3 and 4. Hematite was precipitated as $Fe(OH)_3$ insoluble product in the leachate. This is an indication that the leaching of Cu from the gangue in the ore was selective. This finding corroborated that reported by Ekmekyapar et al. (2003) on leaching of malachite with the lixiviant.

4. Conclusions

The near infrared sensor-based pre-concentration led to the discrimination and classification of the copper ore according to Cu grade and gangue. QEMSCAN® and XRD mineralogical analysis indicated

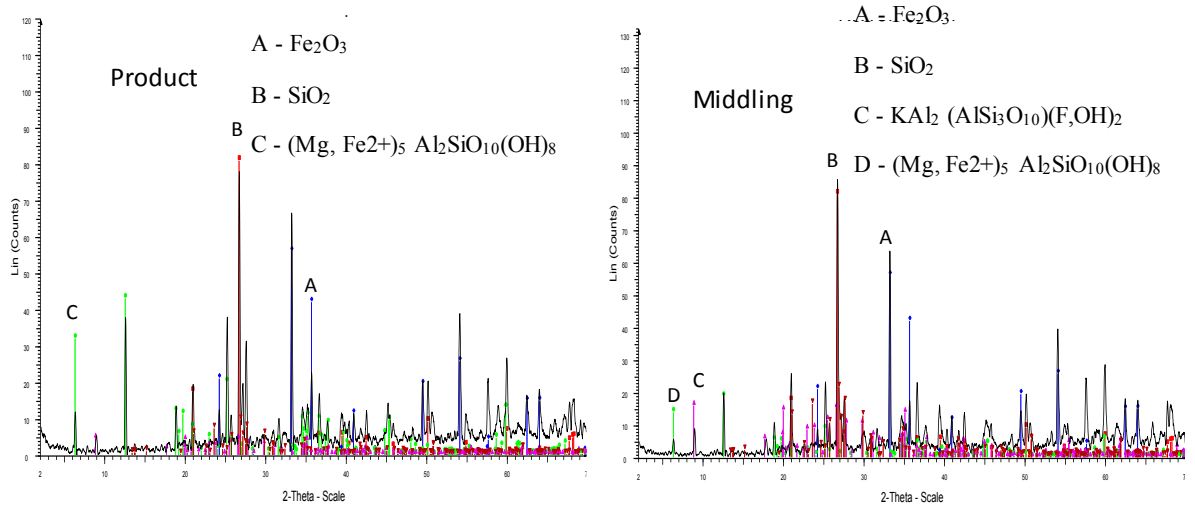

Fig. 18. XRD profiles of residue

good correlation in the determination of minor and major mineral. The major copper-bearing mineral in the ore is chrysocolla. XRF and ICP-MS analysis indicated variation in elemental abundances of elements corresponding to the NIR pre-concentration classification. ICP-MS analysis indicates near complete digestion of metals in aqua regia, thus, suggesting good leaching potential of the ore. SEM analysis revealed the porous nature of the ore. It was also found that Cu metal in the chrysocolla mineral is finely disseminated in the ore matrix and masked by hematite mineral. Therefore, the ore required fine grinding for effective leaching.

It was found also that the leaching rate increases with increase in NH_4Cl concentration, temperature, with decrease in particle size and stirring speed and solid to liquid ratio with higher extraction obtained in the product. This result is consistent with that obtained by Ekmekyapar et al. (2012) and Liu et al. (2010) Künkül et al. (2013) for the alkaline leaching of copper ores. Investigation of the leaching kinetics indicated that the shrinking core model can be used to describe the dissolution rate. The reaction mechanism of dissolution of Cu is controlled by chemical reaction through the particle surface, which is supported by the calculated activation energies of 45.9 Kj/mol and 47.5 Kj/mol (product and middling). The variation in the values between the two classified ore is attributed to the variation in mineral content with the gangue responsible for the trend in behaviour.

Minerals such hematite, quartz, muscovite and clinochlore found in the XRD profile of residue and trace levels of associated metals such as Fe, Mn, Co, Ni, Zn and Pb indicated that NH_4Cl leaching was selective for Cu. This is an indication of less consumption of reactant during the leaching process.

References

AWE, S.A., 2013. *Antimony recovery from complex copper concentrates through hydro-and electrometallurgical processes*. Doctoral thesis, Luleå University of technology, SE-97187 Luleå, Sweden. Pp. 2-20.

AWE, S.A., SANDSTRÖM, Å., 2010. *Selective leaching of arsenic and antimony from a tetrahedrite rich complex sulphide concentrate using alkaline sulphide solution*. Miner. Eng., *23*(15), 1227-1236.

AYDOGAN, S., ARAS, A., CANBAZOGLU, M., 2005. *Dissolution kinetics of sphalerite in acidic ferric chloride leaching*. Chemical Engineering Journal. 114, 67-72.

BABA, A.A., ADEKOLA, F.A., 2010. *Hydrometallurgical processing of a Nigerian sphalerite in hydrochloric acid: Characterization and dissolution kinetics.* Hydrometallurgy, *101*(1), 69-75.

BABA, A.A., AYINLA, K.I., ADEKOLA, F.A., BALE, R.B., GHOSH, M.K., ALABI, A.G.F., Sheik, A.R., FOLORUNSO, I.O., 2013. *Hydrometallurgical application for treating a Nigerian chalcopyrite ore in chloride medium: Part I. Dissolution kinetics assessment.* International Journal of Minerals, Metallurgy, and Materials, *20*(11), 1021-1028.

BINGÖL, D., CANBAZOĞLU, M. 2004. *Dissolution kinetics of malachite in sulphuric acid.* Hydrometallurgy, *72*(1), 159-165.

BINGÖL, D., CANBAZOĞLU, M., AYDOĞAN, S., 2005. *Dissolution kinetics of malachite in ammonia/ammonium carbonate leaching.* Hydrometallurgy, *76*(1), 55-62.

CHMIELEWSKI, T., WÓDKA, J., AND IWACHÓW, Ł., 2009. *Ammonia pressure leaching for lubin shale middlings.* Physicochemical Problems of Mineral Processing, *43*, 5-20.

EKMEKYAPAR, A., OYA, R., KÜNKÜL, A., 2003. *Dissolution kinetics of an oxidized copper ore in ammonium chloride solution.* Chemical and biochemical engineering quarterly, *17*(4), 261-266.

EKMEKYAPAR, A., AKTAŞ, E., KÜNKÜL, A., DEMIRKIRAN, N., 2012. *Investigation of leaching kinetics of copper from malachite ore in ammonium nitrate solutions.* Metallurgical and Materials Transactions B, *43*(4), 764-772.

FILIPPOU, D., ST-GERMAIN, P., GRAMMATIKOPOULOS, T., 2007. *Recovery of metal values from copper-arsenic minerals and other related resources.* Mineral Processing and Extractive Metallurgy Review. 28, 247-298.

IYAKWARI, S., GLASS, H.J. KOWALCZUK, P.B., 2013. *Potential for near infrared sensor-based sorting of hydrothermally-formed minerals.* J. Near Infrared Spectrosc., *21*(3), 223-229.

IYAKWARI, S., HYLKE, J. 2015. *Mineral preconcentration using near infrared sensor-based sorting.* Physicochem. Probl. Miner. Process, *51*(2), 661-674.

IYAKWARI, S., GLASS, H.J., GAVYN, K.R., AND KOWALCZUK, P.B., 2016. *Application of near infrared sensors to preconcentration of hydrothermally-formed copper ore*, Miner. Eng. 85, 148-167

KÜNKÜL, A., GÜLEZGIN, A., DEMIRKIRAN, N., 2013. Investigation of the use of ammonium acetate as an alternative lixiviant in the leaching of malachite ore. *Chemical Industry and Chemical Engineering Quarterly*, *19* (1), 25-34.

LAROUCHE, P., 2001. *Minor elements in copper smelting and electrorefining*. Master thesis, Mining and Metallurgical Engineering, McGill University, Montreal, Canada, pp. 8-12.

LEVENSPIEL, O.,1999. *Chemical reaction engineering*. Industrial & engineering chemistry research, *38* (11), 4140-4143.

LIU, W., TANG, M.T., TANG, C.B., HE, J., YANG, S.H., YANG, J.G., 2010. *Dissolution kinetics of low grade complex copper ore in ammonia-ammonium chloride solution.* Transactions of the Nonferrous Metals Society of China, 20(5), 910-917.

LIU, Z.X., YIN, Z.L., HU, H.P., CHEN, Q.Y., 2012b. *Leaching kinetics of low-grade copper ore with high-alkality gangues in ammonia-ammonium sulphate solution.* Journal of Central South University, *19*, 77-84.

MEECH, J.A., PATERSON, J.G., 1980. *The economics of beneficiating copper oxide ores prior to leaching*. Engineering and Mining Journal (E&MJ), 181(8), 71-77.

MENA, M., OLSON, F.A., 1985. *Leaching of chrysocolla with ammonia-ammonium carbonate solutions.* Metallurgical Transactions B, 16 (3), 441-448

NORGATE, T., JAHANSHAHI, S. 2010. *Low grade ores–Smelt, leach or concentrate?* Minerals Engineering, 23(2), 65-73.

OCHROMOWICZ, K., JEZIOREK, M., WEJMAN, K., 2014. *Copper (ii) extraction from ammonia leach solution.* Physicochem. Probl. Miner. Process, 50(1), 327-335.

POPESCU, A. M., COJOCARU, A., DONATH, C., CONSTANTIN, V., 2013. *Electrochemical study and electrodeposition of copper (I) in ionic liquid-reline.* Chemical Research in Chinese Universities, 29(5), 991-997.

SUN, X.L., CHEN, B.Z., YANG, X.Y., LIU, Y.Y., 2009. *Technological conditions and kinetics of leaching copper from complex copper oxide ore.* J. of Central South University of Technology, 16, 936-941.

WANG, X., CHEN, Q., HU, H., YIN, Z., XIAO, Z. 2009. *Solubility prediction of malachite in aqueous ammoniacal ammonium chloride solutions at 25 C*. Hydrometallurgy, 99(3), 231-237.

WILLS, B.A., NAPIER-MUNN, T., 2006. *Mineral processing technology: An Introduction to the practical aspects of ore treatment and mineral.* Maryland heights, MO: Elsevier science & technology books, pp. 45-56.

WILLS, B.A., 2011.*Mineral processing technology: An introduction to the practical aspects of ore treatment and mineral recovery.* Butterworth-Heinemann, pp. 34-51.